

Iron $K\alpha$ line intensity from accretion discs around rotating black holes

Andrea Martocchia^{1,2,3} and Giorgio Matt¹

¹*Dipartimento di Fisica, Università degli Studi 'Roma Tre', Via della Vasca Navale 84, I-00146 Roma, Italy*

²*LAS/CNR, Via E. Fermi 21, I-00044 Frascati, Italy*

³*Istituto Astronomico, Università di Roma 'La Sapienza', Via G. M. Lancisi 29, I-00161 Roma, Italy*

Accepted 1996 August 14. Received 1996 August 13; in original form 1996 June 26

ABSTRACT

We calculate the iron fluorescent $K\alpha$ line intensity from an accretion disc orbiting around a maximally rotating black hole and illuminated by an X-ray source located on the hole rotation axis.

We find that the line intensity can be much greater than that obtained from illuminated accretion discs around static black holes. This provides a possible explanation for the large iron line equivalent widths observed in some Seyfert 1 galaxies.

Key words: accretion, accretion discs – black hole physics – line: formation – relativity – galaxies: active – X-rays: galaxies.

1 INTRODUCTION

The *ASCA* observation of the Seyfert 1 galaxy MCG-6-30-15 (Tanaka et al. 1995) has revealed an asymmetry in the iron $K\alpha$ line profile, spectacularly confirming theoretical models which attribute the iron line emission to an accretion disc orbiting around a black hole (e.g. Fabian et al. 1989, Laor 1991, Matt et al. 1992). In other Seyfert galaxies the line also appears to be broad (e.g. Mushotzky et al. 1995, Yaqoob et al. 1995, Eracleous, Halpern & Livio 1995, Iwasawa et al. 1996a; Grandi et al., in preparation; Nandra et al. 1996a) and, even if in most cases the asymmetry in the profile has not been unambiguously revealed owing to insufficient signal-to-noise ratio, the relativistic nature of such broadening is the most likely, representing at present the best, if not unique, explanation (Fabian et al. 1995).

The observed line equivalent width (EW), however, is sometimes significantly greater (2–3 times: Nandra et al. 1996a) than expected for an accretion disc orbiting around a static black hole, i.e. 160 eV when the disc is observed face-on (Matt et al. 1992), provided that the illuminating source emits isotropically and that the element abundances are solar (using the abundances of Morrison & McCammon 1983: if those of Anders & Grevesse 1989 are used instead, the value becomes ~ 200 eV – Reynolds, Fabian & Inoue 1995). This value is only slightly greater than that obtained for a semi-infinite slab without any kinematic and relativistic correction (150 eV with Morrison & McCammon abundances: George & Fabian 1991, Matt, Perola & Piro 1991). Greater values for the line EW can be obtained if the primary source emits preferentially towards the disc (e.g.

Ghisellini et al. 1991, Haardt 1993), if the matter is significantly ionized (Matt, Fabian & Ross 1993) or if the iron abundance is greater than solar (e.g. Basko 1978, George & Fabian 1991; Matt, Fabian & Reynolds 1996).

Anisotropic primary emission is distinctly possible and indeed probable, but it is unclear whether or not it could produce a large effect. Matter could be significantly ionized in some sources (Nandra et al. 1996b), but in the majority of objects, including those with the best evidence in favour of relativistic broadening, the line energy is close to 6.4 keV, which indicates that the line photons are emitted by neutral or low-ionization iron atoms. Finally, it should be noted that there are large uncertainties in the atomic data, which could also affect the calculated EW. However, different choices of data sets have generally led to a reduction of the equivalent width (Życki & Czerny 1994; van Teeseling, Kaastra & Heise 1996).

In the present paper we propose a different explanation for the EW enhancement.¹ If the primary source (assumed isotropic in its reference frame) is very close to the black hole, a fraction of photons emitted towards infinity can be deflected by the black hole gravitational field and come back to illuminate the accretion disc, so both increasing the number of X-rays able to produce line emission and reduc-

¹After we started working on this project, we became aware of a work by Fabian et al. (in preparation; see also Fabian 1996) on the line enhancement due to the returning radiation (Cunningham 1976). Their work is in some way complementary to ours, as we are dealing with photon trajectories *before reaching* the disc, while Fabian et al. deal with photon trajectories *after leaving* the disc.

ing that of the primary radiation observed at infinity. For static black holes this effect is counterbalanced by the loss of solid angle subtended by the matter to the source when the latter is very close to the black hole. In fact, the last stable orbit of an accretion disc around a static (Schwarzschild) black hole is 6 (hereinafter all distances are expressed in units of $m \equiv GM/c^2$, i.e. the black hole mass in geometrical units, sometimes called the gravitational radius), and how the matter is distributed within this radius has never, to our knowledge, been studied in detail. On the contrary, for a rotating (Kerr) black hole the innermost stable orbit can be as low as 1 (Bardeen, Press & Teukolsky 1972). We will show that in this case the increase in the line intensity can be significant (up to a factor \sim a few), and that the increase in the equivalent width can be even more dramatic.

2 DISC ILLUMINATION IN A KERR BLACK HOLE

We assume an optically thick, geometrically thin accretion disc corotating with the black hole. Its innermost stable orbit is given by (Bardeen, Press & Teukolsky 1972)

$$r_{\text{ms}} = 3 + Z_2 - [(3 - Z_1)(3 + Z_1 + 2Z_2)]^{1/2}, \quad (1)$$

where

$$Z_1 = 1 + (1 - a^2)^{1/3}[(1 + a)^{1/3} + (1 - a)^{1/3}]; \quad (2)$$

$$Z_2 = (3a^2 + Z_1^2)^{1/2}. \quad (3)$$

Here $a \equiv J/M$ is the normalized angular momentum. In the following we will assume a maximally rotating black hole ($a = 0.9881$, $a = 1$ being prevented by the capture of photons by the hole: Thorne 1974), and therefore $r_{\text{ms}} = 1.232$. Finally, if r is the radial coordinate of the disc, and introducing, for a generic variable x , the function $\Delta(x) \equiv x^2 - 2x + a^2$, the (Keplerian) velocity of the matter in the local non-rotating frame is given by (Bardeen et al. 1972)

$$V_{\text{Kepl}} = \frac{r^2 - 2ar^{1/2} + a^2}{\Delta^{1/2}(r)(r^{3/2} + a)}. \quad (4)$$

We also assume that the primary source is static and located at a distance h on the black hole symmetry axis. There are no reasons why all the emitting particles should be on this axis and, above all, should be static. However, these assumptions greatly simplify the calculations and are possibly representative of a more realistic situation such as a spherical, optically thin corona.

A comprehensive description of the adopted formalism and the relevant equations can be found elsewhere (Martocchia & Matt, in preparation). Here we recall only the most relevant formulae.

Introducing the *Boyer–Lindquist* coordinates t , ξ , θ and ϕ , the projection of the photon trajectory on the ξ – θ plane is determined by the equation of motion (Carter 1968)

$$\int_r V_{\xi}^{-1/2} d\xi = \pm \int_{\theta} V_{\theta}^{-1/2} d\theta, \quad (5)$$

where

$$V_{\xi} = (\xi^2 + a^2 - a\lambda)^2 - \Delta(\xi)[q^2 + (a - \lambda)^2];$$

$$V_{\theta} = q^2 - \cos^2 \theta (\lambda^2 \sin^{-2} \theta - a^2), \quad (6)$$

(see below for the meaning of q and λ). The initial conditions for each trajectory are the distance h and the emission angle δ (in the disc matter reference frame), the latter being given by (Martocchia & Matt, in preparation)

$$\cos \delta = \pm \frac{V_{\xi}^{1/2}(\xi = h)}{h^2 + a^2}. \quad (7)$$

The choice of the symmetry axis ($\theta = 0$) for the emitting point permits us to set one of the four constants of motion, namely λ (which represents the component along the rotation axis of the angular momentum), equal to zero (Carter 1968). The other three constants of motion are the energy, the mass, which is of course null for a photon, and Carter's constant q^2 . As we are interested here only in the photons illuminating the disc, we can consider only those trajectories with Carter's constant greater than zero (Carter 1968).

Equation (5) has been solved numerically. For each photon, the incident angle δ_{inc} and energy shift $g_r \equiv E/E_0$, when reaching the disc, are given by

$$\cos \delta_{\text{inc}} = \frac{|q|}{rg_r} \sqrt{\frac{\Delta(h)}{h^2 + a^2}}, \quad (8)$$

$$g_r = \sqrt{\frac{\Delta(h)(r^2 + a^2 + 2a^2r^{-1})}{(1 - V_{\text{Kepl}}^2)\Delta(r)(h^2 + a^2)}}. \quad (9)$$

Then, the local line emissivity has been computed using the results of Matt et al. (1991), based on Monte Carlo simulations. The local emissivity is weighted by the factor $f_g = g_r^{1.9}$ (~ 1.9 being the canonical photon power-law index for a Seyfert 1 galaxy: Nandra & Pounds 1994) to take into account the fact that the spectrum, as seen by the matter, is shifted in energy, with a consequent change in the number of photons above 7.1 keV, the K-shell photoionization threshold for neutral iron atoms.

3 LINE INTENSITY AND EQUIVALENT WIDTH

In Fig. 1 we present the line intensity I_K emitted by the disc as a function of h for four values of the minimum emitting radius of the disc, r_{min} (namely 1.23, i.e. the last stable orbit, 2, 4 and 6; the outer radius has been taken equal to 1000). We have explored also very small values of h (down to $h = 2$), even if the stability of a source so close to the black hole is rather questionable. The intensities obtained have been divided by the 'classical' value, i.e. the value that is obtained when using a semi-infinite slab illuminated by an isotropic source and without any relativistic and kinematic effect. The value in the figure actually represents an upper limit to the visible enhancement, as, especially for the innermost radii, a substantial fraction of photons are trapped by the black hole or by the disc itself (see below). For simplicity, the intensity is integrated over the emitting solid angle in the matter reference frame. As can be seen from the figure, the line intensity can be as high as 4 times the classical value, and is in any case greater than the classical value for h up to ~ 20 . This enhancement is basically due to three reasons.

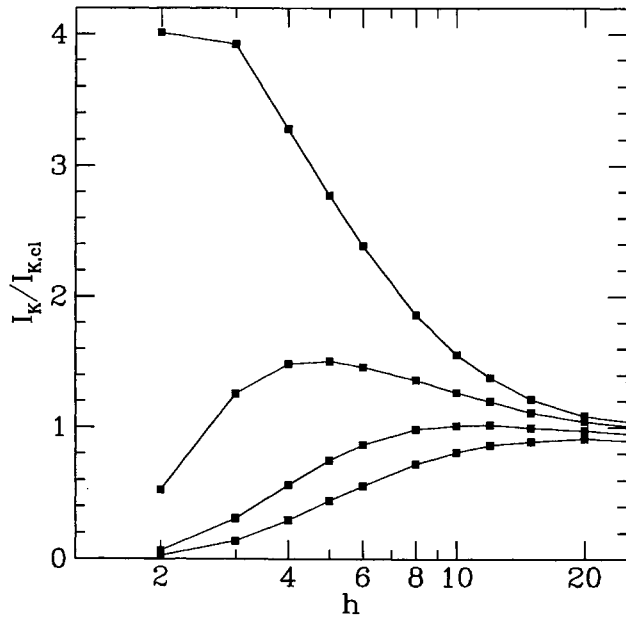


Figure 1. The line intensity emitted by the disc, normalized to the ‘classical’ value (see the text) as a function of h , for four different values of the inner disc radius: 1.23 (the innermost stable orbit), 2, 4 and 6 (from top to bottom). The observable enhancement is somewhat smaller due to photon trapping, as mentioned in the text.

(a) The fraction of primary photons reaching the disc is increased by the light deflection caused by the black hole. Of course, this effect increases with decreasing h .

(b) If $r \lesssim h$, g_r is greater than unity, i.e. photons are blue-shifted and a fraction of photons emitted at h with energies below the photoionization threshold are seen by the matter with energies above the threshold. This increase in g_r is due to both the difference in the gravitational potential between the two points and the rotation of the matter. Of course, at great radii g_r is less than 1 but, at least for small h , these values of the radius have minor importance because of light deflection.

(c) Photons arrive at the disc preferentially with high incident angles (e.g. Cunningham 1976, Martocchia & Matt, in preparation). The efficiency of line emission increases with this angle (e.g. Matt et al. 1991).

The equivalent width, i.e. the ratio between the line flux and the continuum specific flux at the line energy, is further enhanced by the decrease of the primary continuum due both to the decreasing fraction of primary photons reaching infinity, and the gravitational redshift which decreases the specific flux at 6.4 keV. Calling g_h the ratio between emitted and observed photon energies, we have

$$g_h = \sqrt{\frac{\Delta(h)}{h^2 + a^2}}. \quad (10)$$

The quantity W_K , i.e. the ratio between the total line flux and the primary specific flux at 6.4 keV, normalized to the ‘classical’ value, is shown in Fig. 2. For $h=2$, W_K can be as high as 100 times the classical value. However, this quantity is not actually the observed equivalent width. First, the

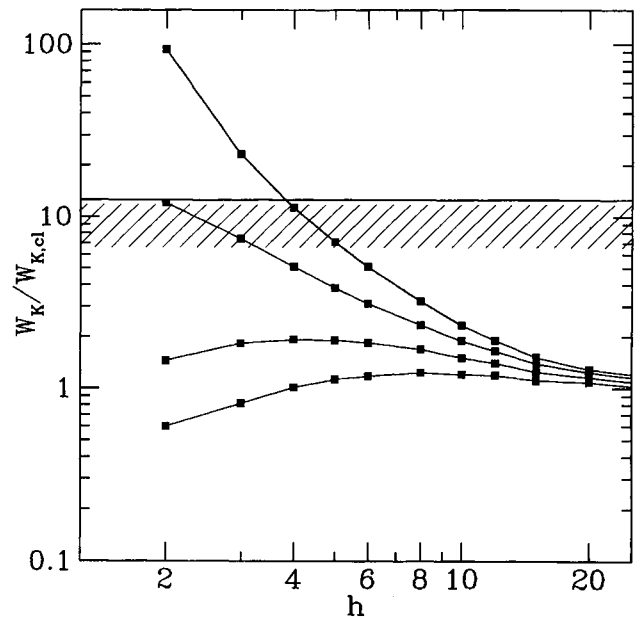


Figure 2. The EW with respect to the primary continuum, normalized to the ‘classical’ value, as a function of h . Curves are as in Fig. 1. The shaded area indicates the maximum value when the Compton reflection continuum is taken into account.

X-ray illumination of the matter produces not only an iron line but also a Compton reflection continuum (e.g. Lightman & White 1988), which in the first approximation increases together with the line (in the classical case, it is about 10 per cent of the primary flux). When the illumination is such that the reflection continuum dominates over the primary one, the line EW can no longer increase, as an increase in the line flux is accompanied by a similar increase in the continuum. Therefore, the maximum observable value of the line EW is about 1–2 keV (Matt et al. 1991; Reynolds et al. 1994), i.e. about 10 times the classical value (see the shaded area in Fig. 2).

In addition, not all of the emitted line photons can actually reach a distant observer, but a fraction of them are captured by the hole or by the disc itself (Thorne 1974; Cunningham 1975, 1976; Fabian et al., in preparation). A precise calculation of this effect is beyond the scope of this paper, and is deferred to a following paper. A very rough estimate, based on the results of Cunningham (1975), is that up to 2/3 of the photons emitted below $r \sim 2$ can be lost in this way, but the effect becomes rapidly less important. Above $r \sim 2$, this effect should reduce the line emission by no more than 10 or 20 per cent, moreover partly compensated by the extra illumination given by the returning photons themselves. Therefore, returning radiation can reduce but not cancel the observed effect.

Finally, it should be recalled that, as the line enhancement is due to emission from the innermost accretion disc, the profiles are expected to be very broad and redshifted, with the double-horned structure practically disappearing in favour of a hump with a big red tail (Laor 1991). Detailed profiles using the emissivity laws derived from our calculations will be presented in Martocchia & Matt (in preparation).

4 DISCUSSION

The broad iron $K\alpha$ lines observed by *ASCA* in several AGN (e.g. Mushotzky et al. 1995, Tanaka et al. 1995, Nandra et al. 1996a), and explained in terms of emission from a relativistic disc (e.g. Fabian et al. 1989, Laor 1991, Matt et al. 1992, and see Fabian et al. 1995 for the discussion, and rejection, of possible alternative explanations), have sometimes equivalent widths in excess by a factor of 2–3 of that expected from an accretion disc around a Schwarzschild black hole (Matt et al. 1992), which in turn is only slightly greater than the ‘classical’ value (George & Fabian 1991; Matt et al. 1991).

One of the most likely explanations for the high EWs observed in some sources is in terms of iron overabundance with respect to the solar value. An EW of ~ 300 eV requires an iron overabundance, with respect to the elements responsible for the photoabsorption at 6.4 keV, ~ 3.6 or ~ 2.6 , depending on whether Morrison & McCammon (1983) or Anders & Grevesse (1989) abundances are adopted (Matt, Fabian & Reynolds 1996).

Here we propose a different explanation based on the fact that, if the black hole is rotating, a strong and even dramatic increase in the line flux is expected, mainly owing to light deflection and gravitational and kinematic blueshifts. These effects are instead small for static black holes, because in that case the innermost stable orbit of the accretion disc is much greater, i.e. $r_{\text{ms}} = 6$ instead of 1.23.

By far the best example of a relativistic line profile is that provided by the long *ASCA* observation of the Seyfert 1 galaxy MCG-6-30-15 (Tanaka et al. 1995). Iwasawa et al. (1996b) have studied in detail the changes in the profile during this observation. Interestingly, in a phase of deep minimum of the total flux the lineshape was best fitted by a Kerr profile (Laor 1991) with the inner emitting radius r_{min} equal to the last stable orbit for a maximally rotating black hole. The equivalent width was particularly high, ~ 1 keV [which is explained by Iwasawa et al. 1996b as the combined effect of returning radiation, i.e. Cunningham 1975 and Fabian et al. (in preparation), and iron overabundance]. This value is about a factor of 3 higher than that obtained with the time-averaged data, which, when fitted with a Kerr profile, gives a best-fitting value for r_{min} of about 9 (Tanaka et al. 1995). A strong increase in EW with decreasing r_{min} is expected in our model (it should be noted that the apparent change of r_{min} could actually reflect a change of h with luminosity). As this increase is at least partly due to the drop in the primary radiation (see Section 3), it is not surprising that the Kerr metric effects appear in a phase of minimum flux. The time-averaged value of EW is in itself greater than expected; with that value of the inner emitting radius no line enhancement is predicted by our model, and it is likely that in this source the iron abundance is actually greater than solar. However, any firm conclusion on the precise value of r_{min} can be derived only by comparing the data with theoretical profiles computed using the proper line emissivity, and subtracting a reflection continuum with the correct intensity and shape (which are also modified by relativistic effects). We are currently calculating such spectra, which will be presented elsewhere (Martocchia & Matt, in preparation).

Another good candidate for hosting a rotating black hole is 3C 120 (Grandi et al., in preparation), where the line is

particularly intense ($EW > 400$ eV) and broad ($\sigma > 0.8$ keV). For this and the other sources with claimed broad lines the signal-to-noise ratio is, however, usually not good enough to permit a direct search for relativistic profiles. Nandra et al. (1996a) have studied in detail the line emission in a sample of 18 Seyfert 1 galaxies observed by *ASCA*. The lines are generally broad, but the details of the profiles cannot in general be revealed. The fits with Schwarzschild and Kerr black holes (with the inner radii set to the respective innermost stable orbit) are equally satisfying. A finer analysis should wait for detectors that combine a high sensitivity with moderate-to-good energy resolution, like, for example, those on board *Spectrum-X-G* and *XMM*.

Indirect checks of our explanation for the large EW observed in some sources are also possible. As the primary X-ray continuum is expected to be significantly redshifted if the emitting region is very close to the black hole, an X-ray luminosity lower than usual (when compared to the optical one) is expected. Moreover, in our model large EW should be accompanied by large amounts of the reflection continuum, which is instead reduced by iron overabundance (George & Fabian 1991; Reynolds et al. 1995). The sensitivity of XTE and SAX up to 100 keV should permit us to constrain, at least in the brightest sources, the amount of the reflection component.

ACKNOWLEDGMENTS

We thank E. Massaro and C. Perola for useful discussions and the referee, A. Laor, for constructive comments.

REFERENCES

- Anders E., Grevesse N., 1993, *Geochim. Cosmochim. Acta*, 53, 197
 Bardeen J. M., Press W. H., Teukolsky S. A., 1972, *ApJ*, 178, 347
 Basko M. M., 1978, *ApJ*, 223, 268
 Carter B., 1968, *Phys. Rev.*, 174, 1559
 Cunningham C. T., 1975, *ApJ*, 202, 788
 Cunningham C. T., 1976, *ApJ*, 208, 534
 Eracleous M., Halpern J. P., Livio M., 1996, *ApJ*, 459, 89
 Fabian A. C., 1996, in *X-Ray Imaging and Spectroscopy of Cosmic Hot Plasmas*. Universal Academic Press, Tokyo, in press
 Fabian A. C., Rees M. J., Stella L., White N. E., 1989, *MNRAS*, 238, 729
 Fabian A. C., Nandra K., Reynolds C. S., Brandt W. N., Otani C., Tanaka Y., Inoue H., Iwasawa K., 1995, *MNRAS*, 277, L11
 George I. M., Fabian A. C., 1991, *MNRAS*, 249, 352
 Ghisellini G., George I. M., Fabian A. C., Done C., 1991, *MNRAS*, 248, 14
 Haardt F., 1993, *ApJ*, 413, 680
 Iwasawa K., Fabian A. C., Mushotzky R. F., Brandt W. N., Awaki H., Kunieda H., 1996a, *MNRAS*, 279, 837
 Iwasawa K. et al., 1996b, *MNRAS*, in press
 Laor A., 1991, *ApJ*, 376, 90
 Lightman A. P., White T. R., 1988, *ApJ*, 335, 57
 Matt G., Perola G. C., Piro L., 1991, *A&A*, 247, 25
 Matt G., Perola G. C., Piro L., Stella L., 1992, *A&A*, 257, 63 (Erratum in *A&A*, 263, 453)
 Matt G., Fabian A. C., Ross R. R., 1993, *MNRAS*, 262, 179
 Matt G., Fabian A. C., Reynolds C. S., 1996, *MNRAS*, submitted
 Morrison R., McCammon D., 1983, *ApJ*, 270, 119
 Mushotzky R. F. et al., 1995, *MNRAS*, 272, L9
 Nandra K., Pounds K. A., 1994, *MNRAS*, 268, 405

Nandra K., George I. M., Mushotzky R. F., Turner T. J., Yaqoob T., 1996a, ApJ, in press
Nandra K., George I. M., Turner T. J., Fukazawa Y., 1996b, ApJ, 459, 542
Reynolds C. S., Fabian A. C., Makishima K., Fukazawa Y., Tamura T., 1994, MNRAS, 268, L55
Reynolds C. S., Fabian A. C., Inoue I., 1995, MNRAS, 276, 1311

Tanaka Y. et al., 1995, Nat, 375, 659
Thorne K. S., 1974, ApJ, 191, 507
van Teeseling A., Kaastra J. S., Heise J., 1996, A&A, in press
Yaqoob T., Edelson R., Weaver K. A., Warwick R. S., Mushotzky R. F., Serlemitsos P. J., Holt S. S., 1995, ApJ, 543, L81
Życki P. T., Czerny B., 1994, MNRAS, 266, 653